Submitted to Journal of
Chemical Physics

LBL-2530
Preprint c.2

LARGE ANGLE INELASTIC SCATTERING OF Na^+ BY D_2

William L. Dimpfl and Bruce H. Mahan

RECEIVED
LAWRENCE
RADIATION LABORATORY

FEB 8 1974

LIBRARY AND
DOCUMENTS SECTION

January 1974

Prepared for the U. S. Atomic Energy Commission
under Contract W-7405-ENG-48

TWO-WEEK LOAN COPY

This is a Library Circulating Copy which may be borrowed for two weeks. For a personal retention copy, call Tech. Info. Division, Ext. 5545

LAWRENCE BERKELEY LABORATORY
UNIVERSITY OF CALIFORNIA
BERKELEY

LBL-2530
c.2

DISCLAIMER

This document was prepared as an account of work sponsored by the United States Government. While this document is believed to contain correct information, neither the United States Government nor any agency thereof, nor the Regents of the University of California, nor any of their employees, makes any warranty, express or implied, or assumes any legal responsibility for the accuracy, completeness, or usefulness of any information, apparatus, product, or process disclosed, or represents that its use would not infringe privately owned rights. Reference herein to any specific commercial product, process, or service by its trade name, trademark, manufacturer, or otherwise, does not necessarily constitute or imply its endorsement, recommendation, or favoring by the United States Government or any agency thereof, or the Regents of the University of California. The views and opinions of authors expressed herein do not necessarily state or reflect those of the United States Government or any agency thereof or the Regents of the University of California.

LBL-2530

LARGE ANGLE INELASTIC SCATTERING OF Na^+ by D_2

William L. Dimpfl and Bruce H. Mahan

Department of Chemistry, and Inorganic Materials Research Division of the Lawrence Berkeley Laboratory, University of California, Berkeley, California 94720

ABSTRACT

We report measurements of the inelasticity of the large angle scattering of Na^+ by D_2, HD, and H_2 in the initial relative energy range 0.74 - 16.9 eV. The interpretation of the vibrational inelasticity leads to the conclusion that perpendicular (C_{2v}) rather than collinear conformations of the Na^+ - D_2 system produce the most intense inelastic scattering. The results of exact classical trajectory calculations which elucidate the effects of oscillator orientation and internal potential function on the inelasticity of collisions are presented. By fitting the calculated inelasticities to the experimental data, we have deduced both the energy and length parameters of a two term exponential repulsive potential for this system.

Ion beam scattering techniques have been notably effective in elucidating the nature of vibrationally inelastic molecular collisions. In the earliest published experiment of this type, Gentry, Gislason, Mahan, and Tsao[1] measured the complete angular distribution of the vibrational-rotational inelasticity in collisions of N_2^+ with He. Subsequent experiments from the same laboratory gave complete velocity vector distributions for the inelastic scattering of O_2^+ and NO^+ by He at a number of initial relative energies.[2] Interpretation of these experiments led to the refined impulse approximation[3] as the correct classical expression for the vibrational inelasticity in collinear collisions near the impulse limit.

Moore and Doering[4] were the first to resolve the excitation of discrete vibrational levels in their experiments on small angle, high energy scattering of H^+ and H_2^+ from H_2, D_2, and N_2. A more extensive investigation of the $H^+ - H_2$ system by Herrero and Doering[5] has since appeared, and these authors also have reported[6] the observation of superelastic collisions of vibrationally excited H_2^+ with several targets. Udseth, Giese, and Gentry[7] measured the differential cross sections for excitation of resolved vibrational states in the $H^+ - H_2$ system at low relative energy (10 eV) and scattering angles smaller than the rainbow angle. Subsequently, a much more extensive investigation of the system has been completed by these authors.[8]

Moran and Cosby[9] reported the detection of vibrational inelasticity in the $Ar^+ - D_2$ system in 1969, and subsequently,

Cosby and Moran,[10] and Petty and Moran[11] published their investigations of the small angle inelastic scattering in the O_2^+ - Ar, O^+ - O_2, and CO^+ - Ar systems. In these studies, the excitation to individual vibrational levels was resolved, and the angular and energy dependence of the inelastic collision probability determined.

The alkali metal ions in collision with H_2, D_2, and HD should be particularly informative systems for the study of collisional inelasticity because both collision partners have closed electronic shells, and all possible electronic excitations and chemical reactions are quite endoergic. Experiments on the large angle scattering of K^+ by H_2 and D_2 were reported by Dittner and Datz[12] in 1968, and a more complete description of these experiments, together with some results on the scattering of Na^+ from H_2 and D_2 were published in a second paper.[13] Van Dop, Boerboom, and Los[14,15] also have studied the scattering of K^+ from H_2 and D_2, with particular emphasis on higher relative energies. Toennies and coworkers[16-18] have made a series of investigations of the scattering of Li^+ by H_2, and in the most recent results, have detected the resolved excitation of H_2 to its first three excited vibrational levels.

In view of the attractive simplicity of the alkali ion-hydrogen molecule systems, and in response to certain apparent differences in the behavior of the Li^+ - H_2 and K^+ - D_2 systems as initially reported,[12,16] we undertook the scattering of Na^+ by D_2 at large angles using an experimental technique differing from that employed by Dittner and Datz[12,13] and Toennies

and coworkers.[16-18] We report our experimental results here, and interpret them in terms of a model which is significantly different from those which have been employed in the past.

Apparatus and Procedure

A diagram of the apparatus used in these experiments is shown in Fig. 1. The ion gun is based on the design of Haskell, Heinz, and Lorents.[19] Ions are emitted from a heated button of alkali alumino-silicate, accelerated, centered and focused onto the entrance aperture of an ion energy selector of the 127° electrostatic deflection type. The latter is similar to the design of Marmet and Kerwin,[20] and employs concentric cylindrical grids (200 lines/in, 60% transmission) to effect the ion deflection. A Faraday cup is positioned directly opposite the entrance aperture of the selector, so that the ion beam intensity before energy analysis can be optimized by adjustment of the ion gun.

The energy selector was operated at a resolution of 3% of the energy of the beam in the selector. The transmission of the selector was satisfactory when the ion energy in the selector was 4 eV or greater. Focusing requirements connected with the subsequent acceleration of the energy selected ions made it impractical to pass the ions through the energy selector at less than 10% of their final laboratory energy in the scattering region. Thus the laboratory energy spread of the unscattered beam was never less than 0.12 eV FWHM.

After leaving the energy selector, the ion beam was accelerated and focused into the scattering cell by a three element aperture lens designed by using the results of Imhof and Read.[21] The scattering cell has fixed entrance and exit apertures, so only scattering at $0° \pm 1.0°$ in the laboratory is observed. The cell was machined from stainless steel and was enclosed by a liquid nitrogen cooled copper jacket. The operating temperature of the cell was -177°C, which considerably decreased the loss in resolution which results from the thermal motion of the scattering gas.

The energy distribution of the ions leaving the scattering cell was measured with an electrostatic energy analyser which was in large measure identical to the ion energy selector. In making a scan of the energy spectrum of the scattered ions, a three element aperture lens was used to accelerate or decelerate ions to a fixed kinetic energy which was passed by the energy analyser. The ions which had been scattered through 180° in the center-of-mass coordinate system were of primary interest, and had lower kinetic energy in the laboratory than the unscattered beam. In early experiments, observation of the back-scattered ions was impeded by a background which resulted from scattering of the primary beam from the outer deflecting grid of the electrostatic energy analyser. To avoid this difficulty, a 25 x 2.5 mm slot was cut in this grid; and this allowed the fast beam ions to leave the deflector region unimpeded. The distortion of the deflecting field which resulted from this slot was minimized by adjusting the potential of another concentric grid of larger radius.

The ions passed by the energy analyser were accelerated into a Bendix Model 4028 Channeltron Electron Multiplier. A nickel mesh was used to prevent penetration of the cathode potential of the multiplier into the energy analyser region. A small flag electrode could be positioned in front of the analyser exit slit, which allowed observation of unscattered beam without overloading the electron multiplier. Pulses from the multiplier were sent to a scaler-teletype system, or to a digital-to-analog converter and X-Y recorder. Elastic scattering from helium was used to calibrate the ion energy scale in the vicinity of 180° scattering in the barycentric system.

The entire ion source, cell, and detection system was mounted on the lid of a 10-inch stainless steel vacuum can. The system was pumped by a 6-inch oil diffusion pump protected by a liquid nitrogen cooled baffle, and was baked at 125°C for 12 hours prior to experiments. This resulted in a pressure of less than 10^{-7} Torr, and stable electrical operation.

Experimental Results

As has been explained in detail a number of times[2,13,16] when a heavy projectile is scattered from a light target gas molecule, a scattering angle of 0° in the laboratory corresponds both to 0° (forward) and 180° (backward) scattering in the center-of-mass coordinate system. The collisions which produce scattering at and near 180° have small impact parameters, and are expected to produce the greatest vibrational inelasticity in a system where the attractive part of the intermolecular potential is weak. Thus, the scattering of Na^+ and D_2

through a barycentric angle of 180° was studied in the relative energy range from 0.74 to 16.9 eV. The value of the inelasticity ΔE at the intensity peak of the energy spectrum of the backscattered Na^+ is given in Table I as a function of the initial relative energy. A few experiments were performed using H_2 and HD as target molecules, and the results of these are also included in Table I. Because of the effects of increased target gas motion, poorer resolution in the barycentric system, and the absence of a convenient target gas to calibrate the energy scale accurately, the results from these last two systems were somewhat less satisfactory than those from the $Na^+ - D_2$ experiments.

In Fig. 2, we show examples of the energy spectra of Na^+ scattered from D_2 at two different initial relative energies. For comparison, the corresponding elastic scattering of Na^+ from He is shown. At the lower initial relative energy of 11.8 eV, Na^+ recoiling from D_2 has its intensity maximum at a laboratory energy slightly greater than the position which corresponds to elastic scattering. Since higher laboratory energies correspond to inelastic scattering in this angular region, the maximum in the curve corresponds to a relatively small inelasticity, 1.1 eV. In addition, comparison of the scattering of Na^+ from D_2 with that from He shows that in the former case there is very significant broadening of the peak in the direction of inelastic scattering.

The inelastic scattering of Na^+ from D_2 is more evident in the data taken at the higher relative energy of 16.30 eV, as

is shown in Fig. 2a. Here both the displacement of the intensity maximum from the value expected for elastic scattering and the asymmetric broadening in the direction of inelastic scattering are quite pronounced. As the initial relative energy is increased still further, both these features become more obvious.

It should be noted that there is a small amount of asymmetric broadening of the distribution of Na^+ scattered by He, even though only elastic scattering can be expected in this case. This effect is attributable to the finite angular resolution of our apparatus, since ions elastically scattered through barycentric angles slightly less than 180° will, if detected, appear to have a larger laboratory velocity and smaller relative velocity than true elastic scattering at 180°.

The inelasticities found in this research are in very good agreement with those reported by Schöttler[22] in the energy range (8 - 17 eV) common to both experiments. This agreement is particularly significant in view of the different experimental techniques used to analyze the scattered ion energy. The inelasticities reported by Dittner and Datz[13] for this system are somewhat greater in the high relative energy (7 - 15 eV) regime than those found in this research and by Schöttler.[22] At lower relative energies, the inelasticities of Dittner and Datz considerably exceed our results and those of Schöttler.

Discussion

In the past, vibrational inelasticity has been discussed in terms of quantum mechanical and classical models which have their

origins in the work of Jackson and Mott,[23] Zener,[24] and Landau and Teller.[25] In these models, it is assumed that an atom A strikes the atom B of a diatomic molecule BC while the system maintains a collinear arrangement throughout the collision. It is also assumed that while the A-B interaction occurs, the BC distance remains constant. This "static oscillator" approximation is also a feature of a more recent model[26] in which collinearity is not assumed. Thus, although the significance of this fact has only fairly recently been recognized,[3] vibrational energy transfer models of the Landau-Teller (L-T) type are based on an impulse approximation to the exact molecular mechanics.

The implicit impulse approximation in L-T models limits the range of mass combinations for which these models are numerically accurate and physically realistic. Kelley and Wolfsberg[27] showed that the mass parameter

$$m = AC/BM$$

was a convenient indicator of the success to be expected from the L-T model. Here A, B, and C stand for the masses of the atoms, and M is the total mass. For values of m greater than 0.25, exact classical trajectory calculations showed that considerable compression of the oscillator occurs during collinear collisions, and the exact energy transferred to vibration was less than that computed using the L-T model. This observation remains valid even when the corrected version of this model,[3] the "refined impulse approximation", is used. For the $Na^+ - D_2$ system, m = 0.8519, so the static oscillator or impulse models of

collinear collisions can not be an adequate basis for discussion of the experimental results of the experiments reported here.

In view of the prevalence of indiscriminate applications of L-T based theories to experimental data, it is worth exploring the following very simple model, which shows clearly why the static oscillator approximation can not be expected to be accurate for systems which have large values of the mass parameter m. The model also leads us to a preferable means of interpreting our experimental data.

As is well-known,[28] the relative kinetic energy T of a collinear triatomic system can be written in the diagonalized form

$$T = \frac{1}{2}\frac{A(B+C)}{M}(\dot{X}^2 + \dot{Y}^2)$$

where the coordinates X and Y are related to the internuclear distances r_{AB}, r_{AC} by

$$X = r_{AB} + \frac{C}{B+C} r_{BC}; \qquad Y = r_{BC}/a$$

$$a^2 = A(B+C)^2/BCM.$$

When X and Y are used as Cartesian coordinates and the potential energy V(X, Y) is plotted in the third dimension, a mass particle sliding without friction on the potential energy surface will execute a motion which is the correct representation of the actual dynamics of the three atom collinear collision. Also, in the X, Y coordinate system, lines of constant r_{AB} and r_{AC} intersect at an internal angle β, which is given implicitly by

$$\tan^2\beta = \frac{BM}{AC} = \frac{1}{m}.$$

Thus the potential energy surface for a diatomic molecule BC bound by a square well potential and interacting with A via a hard sphere potential has the appearance illustrated in Fig. 3a.

The exact trajectory followed by the representative particle for this simple system consists of an initial leg parallel to the X-axis (if initially $\dot{r}_{BC} = 0$), followed by segments generated by specular reflection off the walls as they are encountered. Reference to Fig. 3a shows that when the angle β is large (and m small) the outgoing leg of the trajectory will be nearly parallel to the incoming leg. That is, r_{BC} changes very little during the time that the three atoms are close. This is just the circumstance under which static oscillator or impulse models employing more realistic potential energy surfaces are reasonably accurate. For the hard sphere-square well oscillator system, the geometry of Fig. 3a leads to the following simple expression for the vibrational inelasticity ΔE in terms of the initial relative energy E_r, and the mass distribution parameter β:

$$\frac{\Delta E}{E_r} = \sin^2(2\beta) = \frac{4ABCM}{(A+B)^2(B+C)^2} . \qquad (1)$$

This is also high energy limit of the refined impulse approximation.[3]

One can also see from Fig. 3a that if β is small (m large), the initial A-B interaction will induce a very substantial compressive motion in the oscillator, and this invalidates the impulse models for such systems. In fact, when β is less than 52° ($m > 0.6104$) a second hard sphere interaction between A and B

will occur before the system separates. For even smaller values of β, three or more such interactions will occur as the atom B oscillates between A and C. This multiple collision phenomenon has been discussed by Benson and coworkers,[29] and by Secrest.[30]

The complications of the trajectory that are associated with small values of β are most extreme for the collinear collisions discussed here. However, even for non-collinear collisions, static oscillator models are of doubtful validity when β is small. In these circumstances, the initial interaction of the atoms A and B must immediately induce some form of motion, either vibrational or rotational, in the diatomic BC. Consequently, the forces during the outgoing leg of the trajectory may be quite different from those during the incoming leg, and the static oscillator approximation can not be reliable. Thus, for example, the application[10,11] of the oriented oscillator model of Shin[26] to scattering in the O_2^+ - Ar and CO^+ - Ar systems ($\beta \cong 53°$) seems inappropriate. Since β is 47.3° for the Na^+ - D_2 system, it is clear that a collinear impulse model can not be applied to this system.

There is another factor which precludes the application of Landau-Teller type models to our experimental work. The assumption that the collinear arrangement of atoms leads to the most effective transfer of energy into vibration is not necessarily correct. The recent classical trajectory calculations of Kelley and Wolfsberg[31] show that for zero impact parameter collisions of systems with small values of β, the dependence of the exact inelasticity on the angle between the axis of the diatomic molecule and the relative velocity vector can be quite complicated,

and the inelasticity is not in general a maximum for the collinear arrangement. In addition, there is the important fact that the probability of finding a diatomic molecule oriented such that its axis makes an angle θ with the direction of the relative velocity vector is proportional to $\sin\theta$. Consequently, collinear and near collinear collisions occur most infrequently. Thus if collisions in which θ is near 90° (broadside collisions) have associated with them appreciable inelasticity, they may indeed make the dominant contribution to the energy transfer rate.

An indication of the possible importance of broadside collisions with zero impact parameter can be gleaned from a simple hard sphere-square well oscillator model. If the diatomic molecule is homonuclear (B = C) and if the atom A approaches it with zero impact parameter and with the relative velocity vector perpendicular to the molecular axis, then throughout the collision the molecule will maintain this orientation, and the motion can again be described in terms of just the two coordinates X and Y. Let the A-B separation at which their hard sphere repulsion occurs be called d. Then the equation for the repulsive wall between A and B_2 in X-Y space is

$$X^2 + \left(\frac{aY}{2}\right)^2 = d^2$$

where a^2 is defined as in the collinear problem, but for this homonuclear case has the value $4A/(A + 2B)$. The physically significant part of this ellipse is shown in Fig. 3b. In the region of small Y, it is cut off by the finite hard sphere

distance of closest approach of the two B atoms. At larger values of Y, the ellipse may or may not intersect a line of constant Y which corresponds to the outer lip of the oscillator square well potential.

If the diatomic is initially not vibrating, the first leg of the trajectory of a representative particle on this surface is parallel to the X-axis, as indicated in Fig. 3b. Specular reflection of the representative particle occurs when the trajectory reaches the elliptical wall that represents the hard sphere interaction of atom A with the two B atoms. If the slope of the ellipse at this point is $\tan\gamma$, and if there are no further encounters with the elliptical wall, then a simple argument shows that the change in the vibrational energy of the oscillator is given by

$$\frac{\Delta E}{E_r} = \sin^2(2\gamma) \tag{2}$$

which is the exact analog of Eq. (1).

The slope of the ellipse at Y_e, value of Y at the equilibrium internuclear distance of the diatomic molecule, is

$$\tan\gamma = -\frac{4X}{a^2 Y_e} = -\frac{4}{a^2}\left[\left(\frac{d}{Y_e}\right)^2 - \frac{a^2}{4}\right]^{\frac{1}{2}}$$

This expression shows that the excitation energy will be determined by the mass factors contained in the quantity a^2, and in addition, the size of atom A relative to the internuclear separation of the diatomic at the time of impact. This latter point is an important departure from the collinear case, where the size of atom A has no effect on the inelasticity.[27]

From this simple hard sphere model it is possible to deduce that broadside collisions should increase in importance as the relative energy is raised. If the hard sphere size parameter d is regarded as energy dependent, decreasing as the relative collision energy increases, then in the limit of low energy $d/Y_e >> 1$. Consequently, γ approaches 90°, essentially no force is exerted along the axis of the diatomic molecule, and the inelasticity of the collision approaches zero. As the energy is raised, d/Y_e decreases, and γ increases and approaches 135°. At this point $\Delta E/E_r$ will be unity, if multiple collision effects which result from the contraction of the oscillator are avoided. If the initial relative energy and the inelasticity are great enough so that dissociation of the oscillator occurs as a result of the first interaction with A, these multiple collision effects in fact will be avoided. At very high energies, the effective size parameter d will be such that γ approaches 180°, and $\Delta E/E_r$ again tends toward zero. Estimates of the hard sphere parameter for the $Na^+ - D_2$ system suggest that in the range of relative energies employed in our experiment, the fractional inelasticity $\Delta E/E_r$ should be an increasing function of the initial relative energy, while the fractional inelasticity for collinear and nearly collinear collisions should be energy independent in the hard sphere approximation. Thus broadside collisions are very likely to be most important in the higher energy regime.

While the hard sphere models are convenient and valuable guides to the physical description of collisions, an interpretation of the experimental results requires an understanding of

the behavior of the system under a more realistic interaction potential. Accordingly, we have made exact classical trajectory calculations in order to evaluate the inelasticity as a function of relative energy for collinear and broadside collisions. The interaction potential between the external atom A and the diatomic was taken to be

$$V = A'[\exp(-r_{AB}/L) + \exp(-r_{AC}/L)] \tag{3}$$

where A' is an energy parameter, and L is a length parameter. This "dumbbell" potential is perhaps the simplest that has any claim to realism, and has qualitative features which are similar to some displayed by the $Li^+ - H_2$ potential calculated by <u>ab initio</u> SCF techniques.[32] The internal potential energy of the diatomic molecule was taken to be either the harmonic

$$V_{BC} = \frac{1}{2} k(\Delta r)^2$$

or Morse

$$V_{BC} = D\{1 - \exp[-\alpha(\Delta r)]\}^2$$

potential. Here Δr is the deviation of the internuclear distance from its equilibrium value, k is the force constant for hydrogen (5.725 md/Å), D is the dissociation energy (4.748 eV) and α is the standard Morse parameter for hydrogen (1.944 $Å^{-1}$) The calculations were carried out using standard procedures,[27,31] with a step size small enough so that the total energy was conserved to within 0.01%. The initial conditions were such that the target molecule was neither rotating nor had any vibrational motion.

The results of the calculations of the inelasticity as a function of initial relative energy for collinear collisions of Na^+ with D_2 are shown in Fig. 4. The potential parameters chosen for these exploratory calculations were $A' = 384$ eV and $L = 0.247$ Å, values consistent with predictions of Amdur reported by Dittner and Datz.[13] There is a very large difference in the inelasticities displayed by the harmonic and Morse oscillators, an effect which was briefly noted previously by Kelley and Wolfsberg.[27] The origin of this difference is suggested by the complete trajectories displayed in Fig. 5. On the harmonic oscillator surface, the path of minimum potential energy (the adiabatic path) is noticeably curved. Consequently, the initial straight line motion of the representative particle carries it away from the adiabatic path where it experiences forces which lead to compression of the oscillator. The rather soft harmonic repulsion between the two atoms of the D_2 molecule allows this compression and the resulting re-expansion to occur without substantial transfer of energy back into relative translation, and the collision is rather inelastic, although less inelastic than a refined impulse calculation ($\Delta E = 3.3$ eV at $E_r = 10$ eV) would have suggested.

In contrast, the adiabatic path on the Morse oscillator surface is not strongly curved, and small deviations from it produce large increases in the potential energy. Consequently, the trajectory of the representative particle remains close to the adiabatic path, and crosses the equipotential lines at nearly normal incidence. The result is a rather small inelasticity.

It is clear that these effects of the oscillator potential on the inelasticity are apt to be most important for systems in which the mass parameter is large and the relative energy is high, since under these conditions compression of the oscillator during the collision may be most significant.

The results for the calculated inelasticities of broadside collisions are shown in Fig. 6. Two major features are immediately apparent. Over much of the relative energy range, the inelasticities for the Morse oscillator are roughly an order of magnitude greater for the broadside approach than for the corresponding collinear collision of Fig. 4. In addition, the differences between the Morse and harmonic oscillators are not as great as was true for the collinear case, and for the broadside case, the more realistic Morse potential leads to a greater inelasticity than does the harmonic potential.

Also shown in Fig. 6 are the predictions of an approximate analytical model for the inelasticity of broadside collisions with an harmonic oscillator. The model is the direct analog of the refined impulse model for collinear collisions, and is derived in detail in the appendix. While not particularly accurate for the mass combination used here, it can be used effectively to estimate the inelasticities for broadside collisions in which the mass parameter m is small.

The reason for the increased inelasticity associated with the Morse oscillator is evident in the trajectories displayed in Fig. 7. In both the Morse and the harmonic cases, the collision initially forces an expansion of the oscillator as the trajectory nears its turning point at small X. However, due to the relatively

confined oscillation in the harmonic case, some of the energy transferred to the oscillator in the initial stage of the collision is transferred back to translation as the collision partners start to separate. In contrast, as the Morse oscillator expands, it encounters a potential energy which rises rather slowly, and the energy initially imparted to it is retained as kinetic energy and slowly increasing potential energy. The contraction of the oscillator does not occur until the collision partners are well separated, so the return of the oscillator energy to translation is minimized.

The foregoing calculations make obvious the importance to the energy transfer process of collisions in which the diatomic molecule is perpendicular to the relative velocity vector. It is also important to assess the importance of molecular orientations intermediate between perpendicular and collinear. Figure 8 gives the results of calculations in which the impact parameter was kept constant at zero while the initial orientation angle θ between the relative velocity vector and the molecular axis was varied. At each relative energy, a substantial range of inelasticities occurs, and it is clear that the energy transfer reaches a maximum for orientation angles of the order of 15-20°. The inelasticity of collisions in which the orientation angle is near 90° is a substantial fraction of the maximum inelasticity at small orientation angles, and increases in relative importance as the collision energy is raised.

From the results of Fig. 8, one can conclude that the most probable inelastic process in the energy spectrum of Na^+

scattered from D_2 comes from perpendicular collisions. While orientation angles near 20° have the greatest inelasticity, the occurrence of such collisions must be weighted with a small value of $\sin\theta$ (~0.3). More important, however, is the fact that the inelasticity is a rapidly varying function of the orientation angle in this small angle region. Consequently, only a small range of orientation angles contributes to the intensity of this very inelastic scattering. In contrast, the inelasticity is a slowly varying function of orientation angle near $\theta = 90°$, and these large orientation angles have associated with them the largest values of the $\sin\theta$ weighting factor. Thus a considerable range of frequently occurring orientation angles give inelasticities near that associated with perpendicular collisions. Moreover, it is these nearly perpendicular orientations that give scattering to 180° in the barycentric system when the impact parameter is zero. Thus, if the most intense inelastic feature of the back-scattering in the $Na^+ - D_2$ system is to be characterized in terms of a simple two-dimensional picture, a perpendicular orientation-zero impact parameter model is most appropriate.

It is of interest to deduce the values of the potential parameters A' and L of Eq. (3) by reproducing the energy dependence of the most probable inelasticity using the calculations for zero impact parameter perpendicular collisions. The best fit of the calculated inelasticity to the experimental data for the $Na^+ - D_2$ system is shown in Fig. 9. The potential parameters for the curve shown are A' = 150 eV, and L = 0.40 Å. Since completing our work, we have learned that Faubel and Toennies[33]

have analyzed the data of Schöttler[22] by using the same perpendicular collision-zero impact parameter model employed here, and obtain $A' = 100$ eV and $L = 0.454$ Å for the potential energy parameters. The similarity of the conclusions seems quite satisfactory.

The perpendicular collision model provides a way of reproducing the energy dependence of the most probable inelasticity at large barycentric angles, using reasonable potential parameters. It is of interest, therefore, to attempt to reproduce the full inelastic energy spectrum by extending the model. One possible procedure would be to calculate the full angular and energy distribution of the scattering, using complete classical trajectories obtained from a full set of properly weighted initial conditions. However, this procedure would produce far more information than is necessary for comparison with the experimental data, which involve scattering at only one barcentric angle. Consequently, the following more efficient method was pursued.

Consider an initially stationary (nonvibrating, non-rotating) target diatomic molecule. The orientation angle of the molecular axis with respect to a reference line through the molecular center-of-mass and parallel to the initial relative velocity vector is θ, and ϕ is the initial azimuthal angle of the projectile, measured from the plane determined by the aforementioned reference line and the molecular axis. The initial distance of the projectile from the reference line is the impact parameter b. Let $S(\Theta, \varepsilon)$

be the intensity per unit extension in b, θ, and ϕ, of the scattered Na^+ at the laboratory angle Θ and laboratory energy ε. The variables Θ and ε are, of course, functions of b, θ, and ϕ. To calculate the scattered ion energy spectrum at a laboratory angle $\Theta = 0$, the quantity $S(\Theta, \varepsilon)$ as a function of b, θ, and ϕ must be weighted properly and summed over all the values of b, θ, and ϕ which give scattering at $\Theta = 0$ and various particular values of ε which we shall call E_L. The expression

$$\bar{S}(0,E_L) = \int_0^{\infty} \int_0^{2\pi} \int_0^{\pi} S(\Theta,\varepsilon)\ \delta[E_L - \varepsilon(\theta,b,\phi)]\ H[\Delta\Theta - |\Theta(\theta,b,\phi)|] \sin\theta\ d\theta\ d\phi\ b\,db \tag{4}$$

formally accomplishes this summation. Here $\bar{S}(0, E_L)$ is the intensity of Na^+ at a nominal laboratory angle of zero, and a particular laboratory energy E_L. The Heaviside function which has the property

$$H(x) = 1 \qquad x \geq 0$$

$$H(x) = 0 \qquad x < 0$$

is used to symbolize acceptance of only those scattered ions which fall within the angular width $\Delta\Theta$ of the detector, and the Dirac δ-function insures that only events which lead to the laboratory energy E_L are counted.

The intensity distribution $S(\Theta, \varepsilon)$ could be taken from a full calculation of the scattering. However, since this function

is needed only in the vicinity of 180° in the barycentric system, a simplification is possible. For particular values of the impact parameter b and azimuthal angle ϕ, a restricted $S(\Theta, \varepsilon)$ can be obtained from curves of the inelasticity as a function of the orientation angle θ, such as the ones shown in Fig. 8 for $b = 0$, $\phi = 0$. This restricted $S(\Theta, \varepsilon)$ is in fact proportional to the derivative $d\theta/d(\Delta E)$ which can be evaluated from such a curve. If the inelasticity-orientation curves were available for all values of b and ϕ, the full function $S(\Theta, \varepsilon)$ could be constructed. However, examination of sample trajectories shows that only a small range of impact parameters ($0 \leq b \leq 0.15$ Å) gives scattering with the detector band pass at a nominal barycentric angle of 180°. In this small impact parameter range, the inelasticity is quite insensitive to either the impact parameter or azimuthal angle ϕ. For example, at 10 eV initial relative energy, the maximum value of the inelasticity changes in magnitude by less than 10%, and the orientation angle θ at which this maximum occurs changes by less than 10° as the impact parameter varies from zero to 0.15 Å. Changes in the other portions of the inelasticity-orientation angle curve are smaller, and changes which occur at small values of θ are largely compensated by opposite changes in the inelasticity which occur at supplementary values of θ.

Since inelasticity is insensitive to ϕ and b for small b, Eq. 4 can be replaced by

$$\bar{S}(0, E_L) = C\left(\frac{v}{u}\right)^2 \int_0^{\pi} S(\varepsilon)\, \delta[E_L - (\theta)] \sin\theta \, d\theta \qquad (5)$$

where $S(\varepsilon)$ is evaluated using trajectories for which ϕ and b are both zero. The constant C contains a partial cross section term and the laboratory angular resolution. The square of the ratio of the final laboratory velocity v of Na^+ to its final velocity u in the barycentric systems enters as a result of accounting for the change in the angular bandpass in the barycentric system as the inelasticity varies. When calculated numerically, $\bar{S}(0, E_L)$ has the appearance of a histogram, since the inelasticity was calculated from a set of trajectories in which initial values of θ spaced by 2.5° were used. This histogram, which assumes effectively infinite energy resolution at the detector as well as no target gas motion or beam energy spread, must be convoluted with an apparatus energy resolution function before being compared with experimental data. To effect this convolution, an apparatus function derived from the experimental elastic scattering from He was used.

To find an optimum set of potential energy parameters, an energy spectrum calculated using assumed values for A' and L was compared with experimental data, appropriate adjustments to the parameters made, and the calculations and comparison repeated. Figure 10 shows examples of the results of this fitting procedure. In the right hand panels, the histograms obtained from the trajectory calculation are shown. In the left hand panels, the experimental data appear together with the apparatus resolution function and the calculated fit to the experimental data. With a single set of potential parameters, it was not possible to fit the scattered ion energy spectrum exactly over the full range of

initial relative energies. The parameters used in the calculations of Fig. 10 (Λ' = 65 eV, L = 0.55 Å) represent a compromise which fits both the intensity maximum and the inelastic tail reasonably well over the full experimental range of initial relative energies. The most apparent discrepancy between the calculation and experimental data occurs in the region of the inelastic tail. Intensity in this very inelastic region results from collisions in which the orientation angle θ is of the order of 20°. Use of a smaller value of the range parameter improves the fit in this region, which suggests that the interaction potential is slightly stiffer for collinear than for perpendicular conformations.

It should also be mentioned that a fit to experimental data was obtained from a set of calculations in which the impact parameter b as well as the orientation angle θ was varied. The convoluted energy spectrum from the full two-dimensional calculation was virtually indistinguishable from the calculations using only a zero impact parameter. Consequently, the simpler procedure seems justified.

Figure 11 shows a comparison of the calculated and experimental inelastic spectrum for Na^+ - HD collisions. The potential parameters used were those derived from the best fit to the Na^+ - D_2 data. Generally quite satisfactory agreement between the calculations and experiment is obtained, although the deviations in the regions of the inelastic tail are quite noticeable at the higher relative energies. There are rather significant differences between the mechanics of Na^+ - D_2 and Na^+ - HD collisions. Nearly collinear collisions in which the

atomic arrangement is Na^+ - HD are very inelastic, appreciably more so than the nearly collinear Na^+ - D_2 collisions. Consequently, the very inelastic tail is more prominent in the Na^+ - HD experiments. Nearly collinear collisions of the type Na^+ - DH have only slightly greater inelasticity than do exact perpendicular collisions, and consequently contribute to the spectrum in the region of the intensity peak. The fact that despite these differences in the mechanics of the D_2 and HD systems the same potential parameters reasonably reproduce the experimental energy spectra re-enforces confidence in the derived intermolecular potential.

In the model used to fit the experimental data, the zero point oscillation present in real oscillators was ignored. It can be argued that for high energy collisions, this procedure may lead to reasonable results, since it emphasizes the potential energy surface in the region of the equilibrium oscillator distance, as does the weighting derived from the ground state vibrational wavefunction. To explore this problem further, trajectories were run in which the oscillator had the zero point vibrational energy, and several values of the initial vibrational phase were explored. A phase averaged intensity histogram was calculated and compared with one obtained without zero point energy. Differences were evident which could lead in a full analysis to different values of the potential parameters. However, it is not clear that this classical phase averaging procedure is more appropriate than the procedure which we have followed. The question might be answered by testing the effectiveness of the potential we have derived in predicting the appearance of resolved vibrational transitions.

The two sets of potential parameters $A' = 150$ eV, $L = 0.40$ Å and $A' = 65$ eV, $L = 0.55$ Å derived from this work bracket the parameters $A' = 100$ eV, $L = 0.454$ Å found by Faubel and Toennies. Although these three sets of parameters may seem rather different, the potentials to which they correspond are virtually identical in the range 9 - 18 eV, $r_{AB} = r_{BC} = 1.3 - 1.0$ Å. The fractional deviations at large $Na^+ - D_2$ separations tend to be large because the potentials are small in this region. At high energy (>20 eV) and small separations ($r_{AB} = r_{BC} < 1$Å) the potentials deviate again. However, within the relative energy range of our experiments, the three potentials are quite similar. This set of experiments seems to be the first in which both parameters of an exponential repulsive potential have been deduced from vibrationally inelastic scattering.

Acknowledgement: This work was supported by the U. S. Atomic Energy Commission.

APPENDIX

Consider zero impact parameter collisions of an atom A with a homonuclear diatomic molecule B_2 in the perpendicular orientation shown in Fig. 3b. Let the total potential energy be given by

$$V = 2A' e^{-r_{AB}/L} + \frac{1}{2} k(\Delta r)^2$$

where Δr is the deviation of the diatomic internuclear separation from its equilibrium value. Now if X, the separation of the centers-of-mass of A and B, is such that $4X^2 > r^2$, then we can write

$$r_{AB} = (X^2 + \frac{r^2}{4})^{\frac{1}{2}} \simeq X + \frac{r^2}{8X}.$$

The Lagrange equation for the X-motion is in this approximation

$$\tilde{m}\ddot{X} = \frac{2A'}{L} [\exp-(X + \frac{r^2}{8X})/L] \ (1 - \frac{r^2}{8X^2}) \qquad \text{(A1)}$$

where

$$\tilde{m} = 2A\ B/(A + 2B).$$

The last term $r^2/8X^2$ in Eq. (A1) can be dropped, since it is much smaller than unity.

If X_t is the classical turning point, let $x = X - X_t$, and let r_e be the equilibrium separation of the diatomic. In the exponential term of Eq. (A1) let $r^2/8X$ be replaced by $r_e^2/8X_t$. Then the approximate equation for the X motion is

$$\tilde{m}\ddot{x} = \frac{2A''}{L} e^{-x/L} \qquad \text{(A2)}$$

where

$$A'' = A'\exp-[X_t + r_e^2/8X_t]/L$$

or half the potential energy at the turning point. Now Eq. (A2) can be integrated to give

$$e^{-x/L} = \mathrm{sech}^2\,(v_o t/2L) \tag{A3}$$

where v_o is the initial relative velocity.

For the oscillator, the Lagrange equation is

$$\mu(\Delta\ddot{r}) + k(\Delta r) = -\frac{A''}{2L}\frac{(\Delta r + r_e)}{(x + X_t)}\,e^{-x/L} \tag{A4}$$

where $\mu = B/2$, the reduced mass of the oscillator. As a further approximation, set x and Δr to zero in the pre-exponential factor. Straightforward geometric considerations lead to the expression

$$r_e/X_t = -4/(a\,\tan\gamma)$$

where $\tan\gamma$ is the slope of the equipotential at the turning point as used in Fig. 3b, and $a = 4AB/(A + 2B)$. Then Eq. (A4) becomes

$$\mu(\Delta\ddot{r}) + k(\Delta r) = \frac{2A''}{aL}\,\mathrm{ctn}\gamma\,\mathrm{sech}^2\,(v_o t/2L) \tag{A5}$$

Equation (A5) constitutes a driven oscillator problem, so the energy transferred to vibration can be obtained in the usual manner[3] from the square of the Fourier transform of the force. The result is

$$\frac{\Delta E}{E_r} = \left(\frac{16\,\mathrm{ctn}^2\gamma}{a^2\mu\tilde{m}v_o^4}\right)(2A'')^2\left(\frac{\pi\omega L}{v_o}\right)^2 \mathrm{csch}^2\left(\frac{\pi\omega L}{v_o}\right). \tag{A6}$$

But $2A''$ is the potential energy at the turning point, and is given in terms of the initial kinetic energy by

$$2A'' = \frac{1}{2}\,\tilde{m}\,v_o^{\,2}\,\sin^2\gamma.$$

Substitution into Eq. (A6) gives

$$\frac{\Delta E}{E_r} = \sin^2\,(2\gamma)\,\left(\frac{\pi\omega L}{v_o}\right)^2\,\mathrm{csch}^2\cdot\left(\frac{\pi\omega L}{v_o}\right) \tag{A7}$$

which is the exact analog of the refined impulse expression[3] for energy transfer in collinear collisions. However, in the present problem the quantity γ is determined not just by the masses, but by the potential energy surface.

To use Eq. A7, γ must be found. The potential energy at the turning point X_t, r_e is

$$2A'' = 2A'\,\exp[-(X_t + r_e^{\,2}/8X_t)/L] = E_{rel}/(1 + \mathrm{ctn}^2\gamma).$$

Make the substitution

$$r_e/X_t = -4/a\,\tan\gamma)$$

and rearrangement gives

$$X_t = L\,\left[\frac{\ell n(1+\mathrm{ctn}^2\gamma) - \ell n(E_r/2A')}{1 + \dfrac{2\mathrm{ctn}^2\gamma}{a^2}}\right]$$

For small values of $\mathrm{ctn}\gamma$, this becomes

$$X_t = L\left[\frac{\operatorname{ctn}^2\gamma - \ln(E_r/2A')}{1 + \frac{2\operatorname{ctn}^2\gamma}{a^2}}\right]$$

$$\cong -L \ln \frac{E_r}{2A'}$$

which may be solved by successive approximations to give X_t, and then $\tan\gamma$.

REFERENCES

1. W. R. Gentry, E. A. Gislason, B. H. Mahan, and C. W. Tsao, J. Chem. Phys. 47, 1856 (1967).

2. M. H. Cheng, M. H. Chiang, E. A. Gislason, B. H. Mahan, C. W. Tsao, and A. S. Werner, J. Chem. Phys. 52, 6150 (1970).

3. B. H. Mahan, J. Chem. Phys. 52, 5221 (1970).

4. J. H. Moore and J. P. Doering, Phys. Rev. Letters 23, 584 (1969).

5. F. A. Herrero and J. P. Doering, Phys. Rev. A 5, 702 (1972).

6. F. A. Herrero and J. P. Doering, Phys. Rev. Letters 29, 609 (1972).

7. H. Udseth, C. F. Giese, and W. R. Gentry, J. Chem. Phys. 54, 3642 (1971).

8. H. Udseth, C. F. Giese, and W. R. Gentry, J. Chem. Phys. (to be published).

9. T. F. Moran and P. C. Cosby, J. Chem. Phys. 51, 5724 (1969).

10. P. C. Cosby and T. F. Moran, J. Chem. Phys. 52, 6157 (1970).

11. F. Petty and T. F. Moran, Phys. Rev. A 5, 266 (1972).

12. P. F. Ditner and S. Datz, J. Chem. Phys. 49, 1969 (1968).

13. P. F. Ditner and S. Datz, J. Chem. Phys. 54, 4228 (1971).

14. H. van Dop, A. J. H. Boerboom, and J. Los, Physica 54, 223 (1971).

15. H. van Dop, A. J. H. Boerboom, and J. Los, Physica 61, 616 (1972).

16. J. Schöttler and J. P. Toennies, Z. Physik 214, 472 (1968).

17. W. D. Held, J. Schöttler and J. P. Toennies, Chem. Phys. Letters 6, 304 (1970).

18. R. David, M. Faubel, and J. P. Toennies, Chem. Phys. Letters 18, 87 (1973).

19. H. B. Haskell, O. Heinz and D. C. Lorents, Rev. Sci. Instr. 37, 607 (1966).

20. P. Marmet and L. Kerwin, Can. J. Phys. 38, 787 (1960).

21. R. E. Imhof and F. H. Read, J. Sci. Instr. 1, 859 (1968).

22. J. Schöttler, Max Planck Institut für Strömungsforschung, Göttingen, Germany, Bericht 104/72 (1972), unpublished.

23. J. M. Jackson and N. F. Mott, Proc. Roy. Soc. (London) A137, 703 (1932).

24. C. Zener, Phys. Rev. 38, 277 (1931); Proc. Cambridge Phil. Soc. 29, 136 (1932).

25. L. Landau and E. Teller, Physik Z. Sowjetunion 10, 34 (1936).

26. H. K. Shin, J. Phys. Chem. 73, 4321 (1969).

27. J. D. Kelley and M. Wolfsberg, J. Chem. Phys. 44, 324 (1966).

28. J. O. Hirschfelder, Int. J. Quantum Chem. 3S, 17 (1969).

29. S. Benson, G. C. Berend, and J. C. Wu, J. Chem. Phys. 38, 25 (1963).

30. D. Secrest, J. Chem. Phys. 51, 421 (1969).

31. J. D. Kelley and M. Wolfsberg, J. Chem. Phys. 53, 2967 (1970).

32. W. A. Lester, Jr. J. Chem. Phys. 54, 3171 (1971).

33. M. Faubel and J. P. Toennies, private communication 1973.

Figure Captions

Fig. 1 A diagram of the alkali metal ion scattering apparatus. A: Ion source assembly. B: Liquid nitrogen cooled copper clamp. C: Energy analyser. D: Faraday cup. E: Beam flag. F: Channeltron detector. G: Scattering cell. H: Ion energy selector.

Fig. 2 Examples of the energy spectra of Na^+ scattered at a barycentric angle of 180° from D_2 and He. The abscisca is the laboratory energy of the scattered Na^+. The energy scales have been adjusted by the amount indicated by using the calculated position of the elastic scattering from He as a calibration point. The vertical lines indicate the positions expected for elastic scattering, and the suspended tic-marks located positions expected for inelastic scattering to the excited vibrational states of D_2.

Fig. 3 Potential energy surfaces for the collision of a hard sphere atom with a square-well diatomic oscillator. (a) Collinear conformation. (b) Isosceles triangle conformation. For definitions of the symbols, see the text.

Fig. 4 The calculated inelasticity ΔE as a function of initial relative energy E_r for the collinear collisions of Na^+ with D_2. Note that over most of the relative energy range, the inelasticity calculated assuming an harmonic oscillator potential for D_2 is much greater than that calculated assuming a Morse potential function. The external potential energy function is an exponential repulsion with $L = 0.247$ Å.

Fig. 5 Skewed coordinate representations of the collinear collisions of Na^+ with D_2 at 10 eV initial relative energy. The potential energy contours are labeled in eV, taking the zero as the oscillator minimum at infinite atom-diatom separation. The ordinate r is scaled to give the actual internuclear separation of D_2. (a) Harmonic potential function for D_2, inelasticity $\Delta E = 2.07$ eV. (b) Morse potential function for D_2, $\Delta E = 0.17$ eV. In both cases, the exponential repulsion of Eq. 3 is used, with $A' = 384$ eV and $L = 0.247$ Å. The dotted lines locate the adiabatic path on each surface.

Fig. 6 The vibrational inelasticity ΔE as a function of initial relative energy E_r for the collisions of Na^+ with D_2 in the isosceles triangle conformation. Exact results are given for D_2 treated as a Morse and as an harmonic oscillator. The predictions of the approximate refined impulse model described in the Appendix are also given. In all cases the external potential of Eq. 3 was used with $A' = 384$ eV, and $L = 0.247$ Å.

Fig. 7 Exact trajectories for the collisions of Na^+ with D_2 in the isosceles triangle conformation. The ordinate is the actual internuclear separation of D_2, the abscissa is the separation of the centers of mass of Na^+ and D_2. The initial relative energy was 10 eV in both cases, and the external potential energy was that given by Eq. 3 with $A' = 384$ eV and $L = 0.247$ Å. In panel (a), D_2 was taken

to be an harmonic oscillator, and the inelasticity $\Delta E = 1.61$ eV. In panel (b) D_2 is assumed to be a Morse oscillator, and the inelasticity $\Delta E = 2.72$ eV. Note that in the latter case the oscillator does not contract until it is well separated from the ion. The opposite is true in the harmonic case.

Fig. 8 The fractional inelasticity $\Delta E/E_r$ as a function of the orientation angle θ between the D_2 internuclear axis and the relative velocity vector. The impact parameter is zero, the external potential is the same as in Figs. 4-7, and D_2 is taken to be a Morse oscillator. Note that the relative importance of collisions near the perpendicular orientation increases markedly with increasing initial relative energy.

Fig. 9 Exact calculations of the vibrational inelasticity (solid line) for the perpendicular orientation-zero impact parameter collision model fitted to the experimental data for $Na^+ - D_2$ collisions (squares). Deuterium was taken to be a Morse oscillator. The potential parameters of Eq. 3 which give this fit are $A' = 150$ eV and $L = 0.40$ Å.

Fig. 10 The fitting of the complete calculated energy spectrum of scattered Na^+ to the experimental data. (a) Initial relative energy 7.41 eV. In the right hand panel, the histogram gives the distribution of energies of Na^+ calculated from the zero impact parameter collision model with proper weighting of molecular orientations. In the left hand panel, the convolution of the histogram with the apparatus function (Fit) is compared with the experimental data (circles). The curve labeled $Na^+ - He$ is the experimental elastic scattering

from which the apparatus function was taken. (b) A similar analysis for collisions at 13.3 eV initial relative energy.

Fig. 11 The fitting of the calculated energy spectra of Na^+ scattered from HD to the experimental data for two values of the initial relative energy. The notation and procedure are the same as in Fig. 10.

Table 1

Experimental inelasticities for Na^+ backscattered from hydrogen molecules.

Na^+-D_2				Na^+-H_2			
Exp. No.	E_ℓ[a] (eV)	E_r[b] (eV)	ΔE[c] (eV)	Exp. No.	E_ℓ (eV)	E_r (eV)	ΔE (eV)
77a	20.	2.96	0.00	51	30.	2.40	0.23
41	20.	2.96	0.00	53	40.	3.20	0.08
42	25.	3.70	0.00	54	50.	4.00	0.22
77b	30.	4.44	0.00	55	60.	4.80	0.11
38	30.	4.44	-0.01				
37	30.	4.44	0.03				
45	35.	5.19	-0.01				
77c	40.	5.93	0.07	Na^+-HD			
64a	40.	5.93	0.14				
46	40.	5.93	0.11	Exp. No.	E_ℓ (eV)	E_r (eV)	ΔE (eV)
64b	45.	6.67	0.20				
64c	50.	7.41	0.23	71	70.	8.08	0.68
49	50.	7.41	0.00	72	80.	9.23	0.38
64d	55.	8.15	0.27	73	90.	10.38	0.62
59	60.	8.89	0.24	74	100.	11.54	0.69
64e	60.	8.89	0.42	75	110.	12.69	1.22
60	70.	10.37	0.63	78	130.	15.00	2.11
62	80.	11.85	1.10	79	150.	17.31	2.81
68	85.	12.59	1.20	81	190.	21.92	5.79
63	90.	13.33	1.69	80	200.	23.08	7.48
69	90.	13.33	1.53	82	250.	28.85	12.78
70	95.	14.07	2.07				
65	100.	14.81	2.74				
66	110.	16.30	3.46				
67	114.	16.89	3.92				

[a] Initial laboratory energy of Na^+

[b] Initial relative energy

[c] Most probable inelasticity

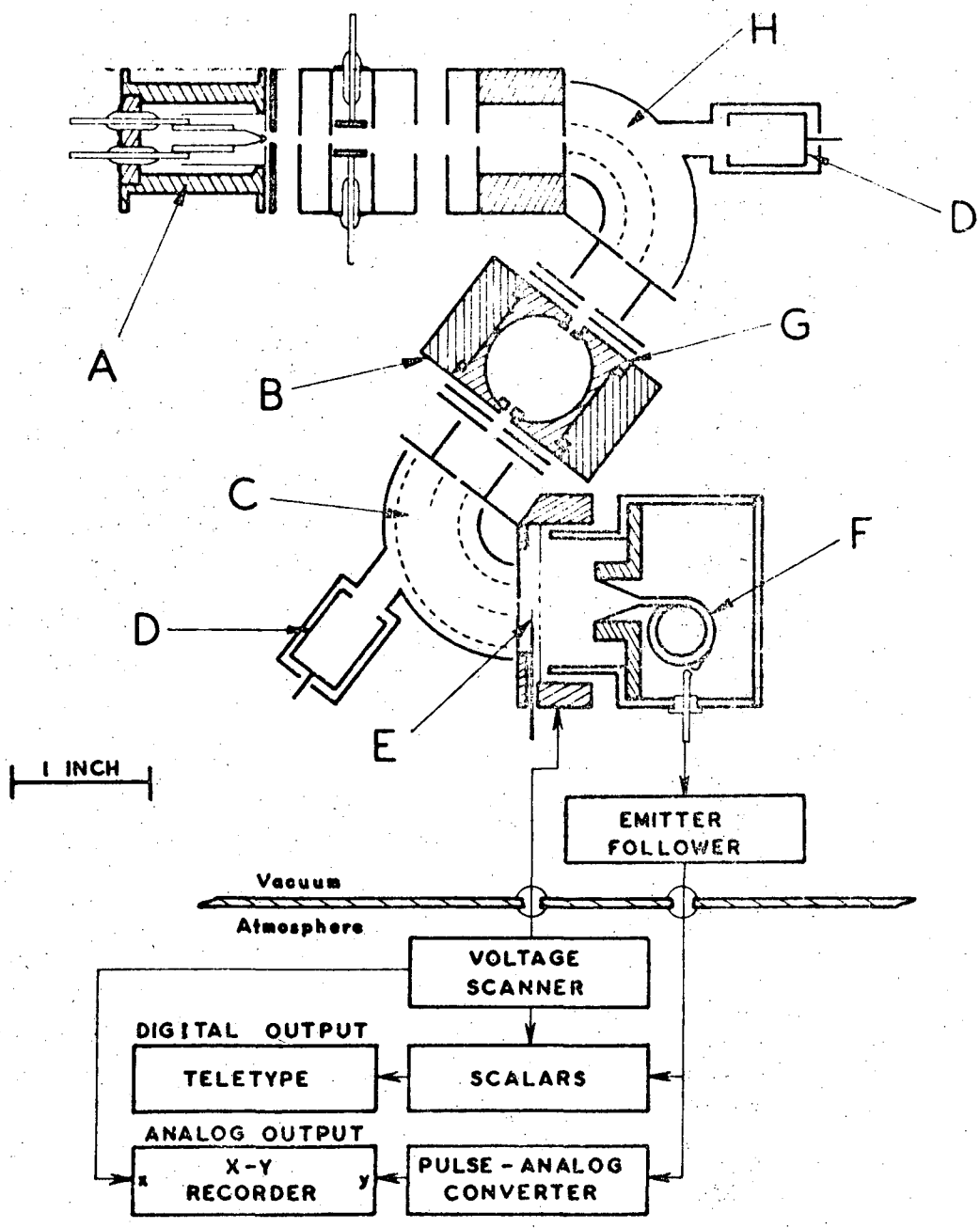

XBL 737-1504

Fig. 1

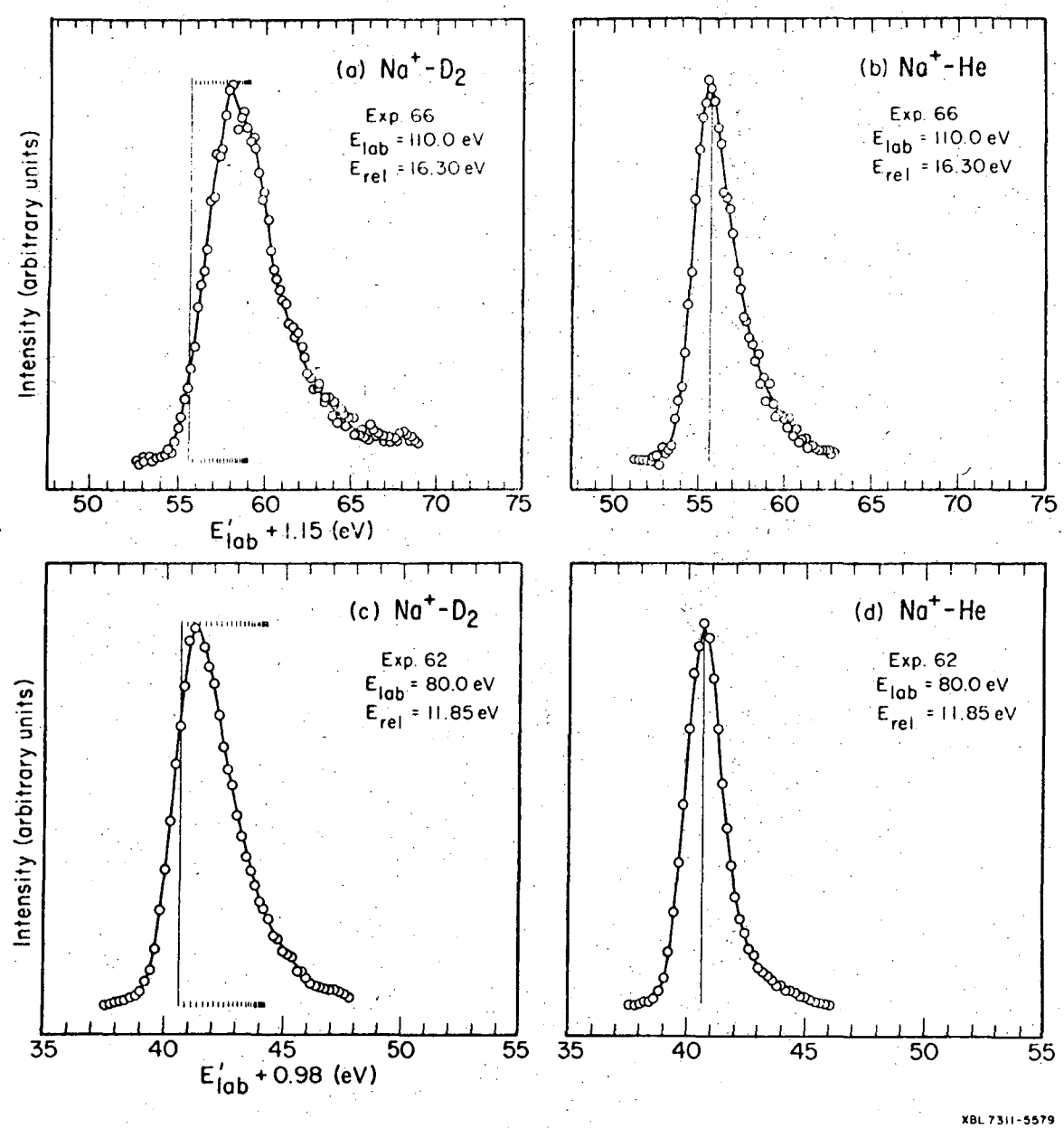
(a) Na+-D2
Exp. 66
Elab = 110.0 eV
Erel = 16.30 eV
(b) Na+-He
Exp. 66
Elab = 110.0 eV
Erel = 16.30 eV
(c) Na+-D2
Exp. 62
Elab = 80.0 eV
Erel = 11.85 eV
(d) Na+-He
Exp. 62
Elab = 80.0 eV
Erel = 11.85 eV
Intensity (arbitrary units)
E'lab + 1.15 (eV)
E'lab + 0.98 (eV)
50 55 60 65 70 75
35 40 45 50 55
XBL 7311-5579

Fig. 2

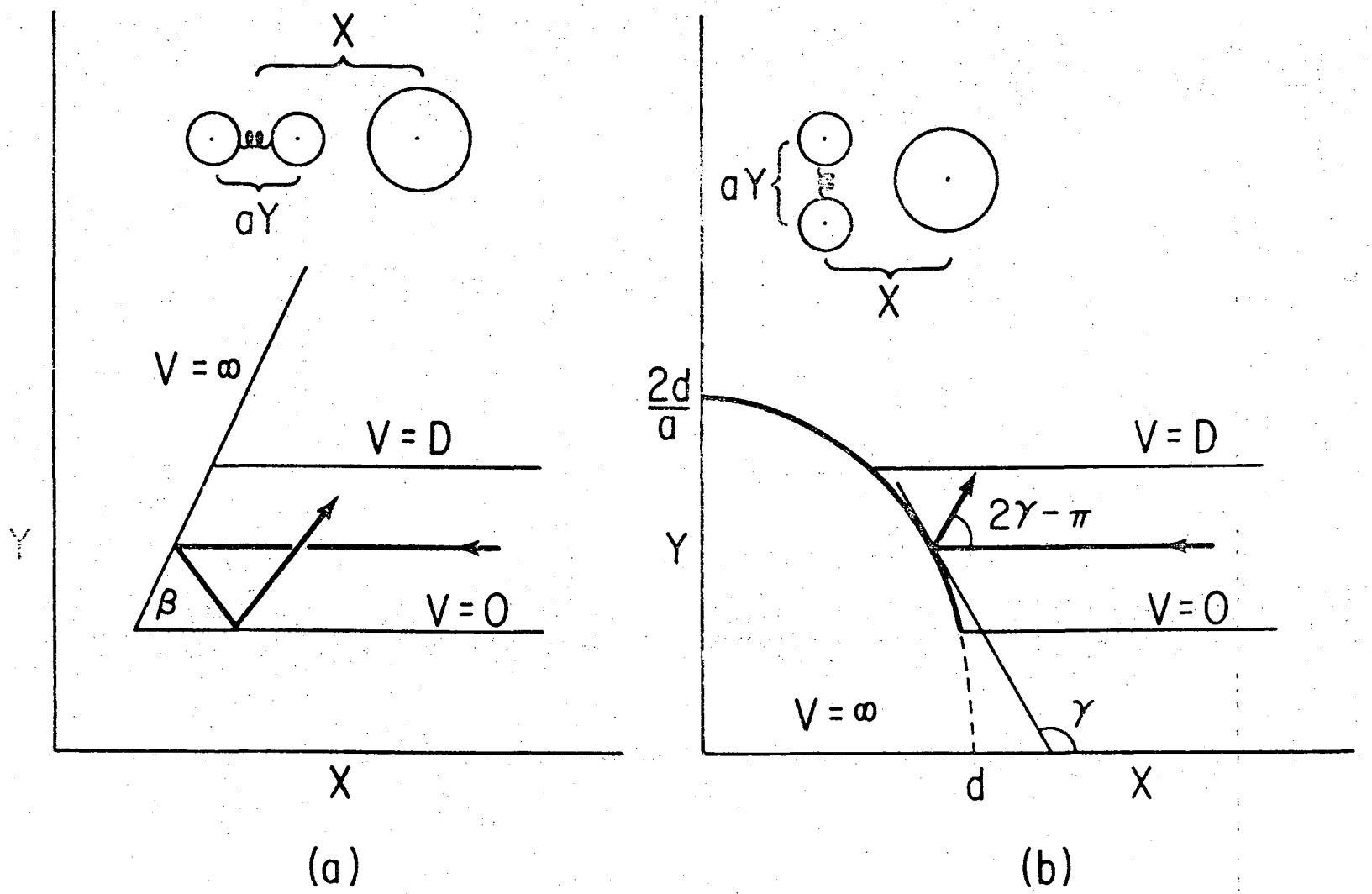

XBL 7311-5581

Fig. 3

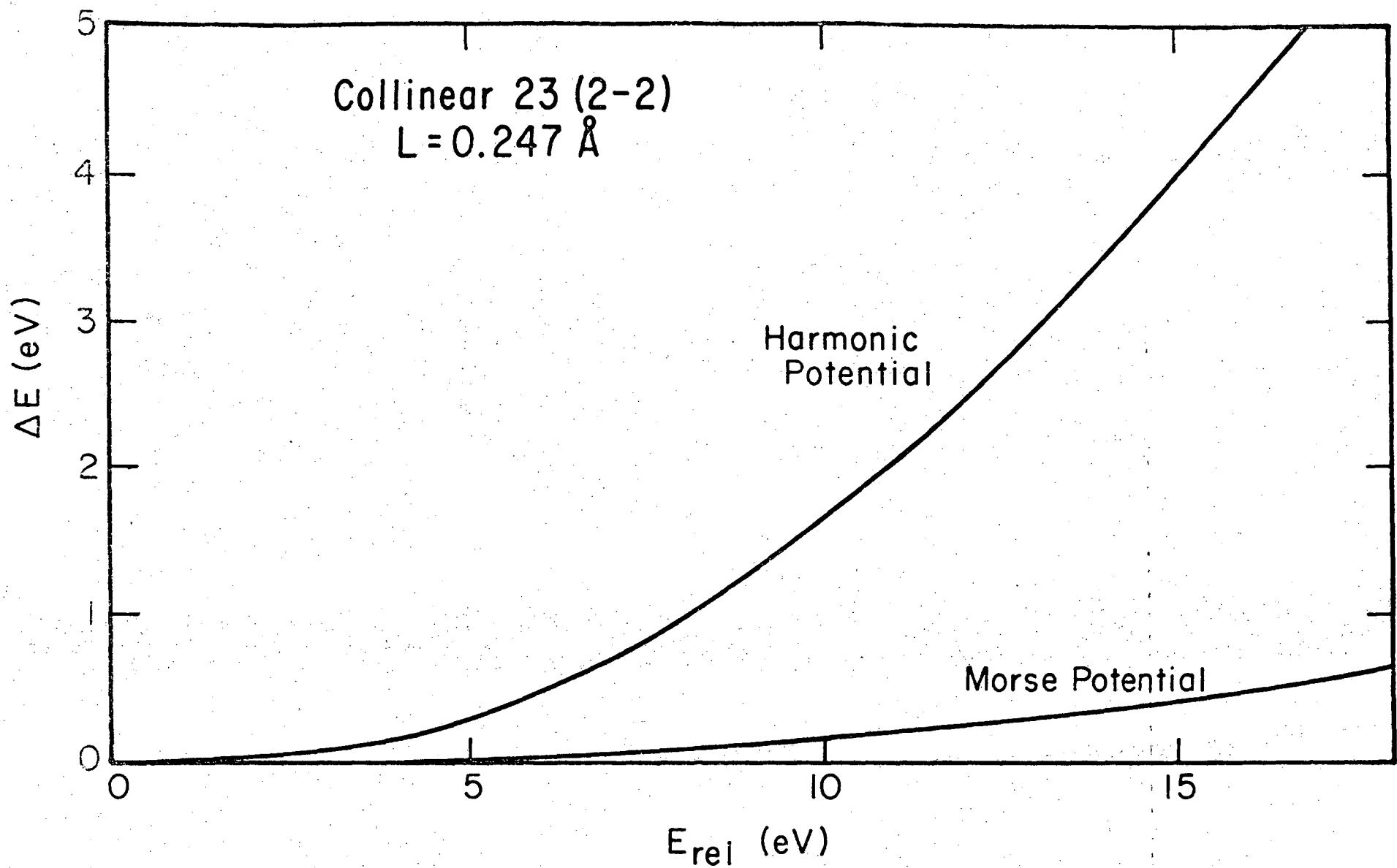

XBL 737-6440

Fig. 4

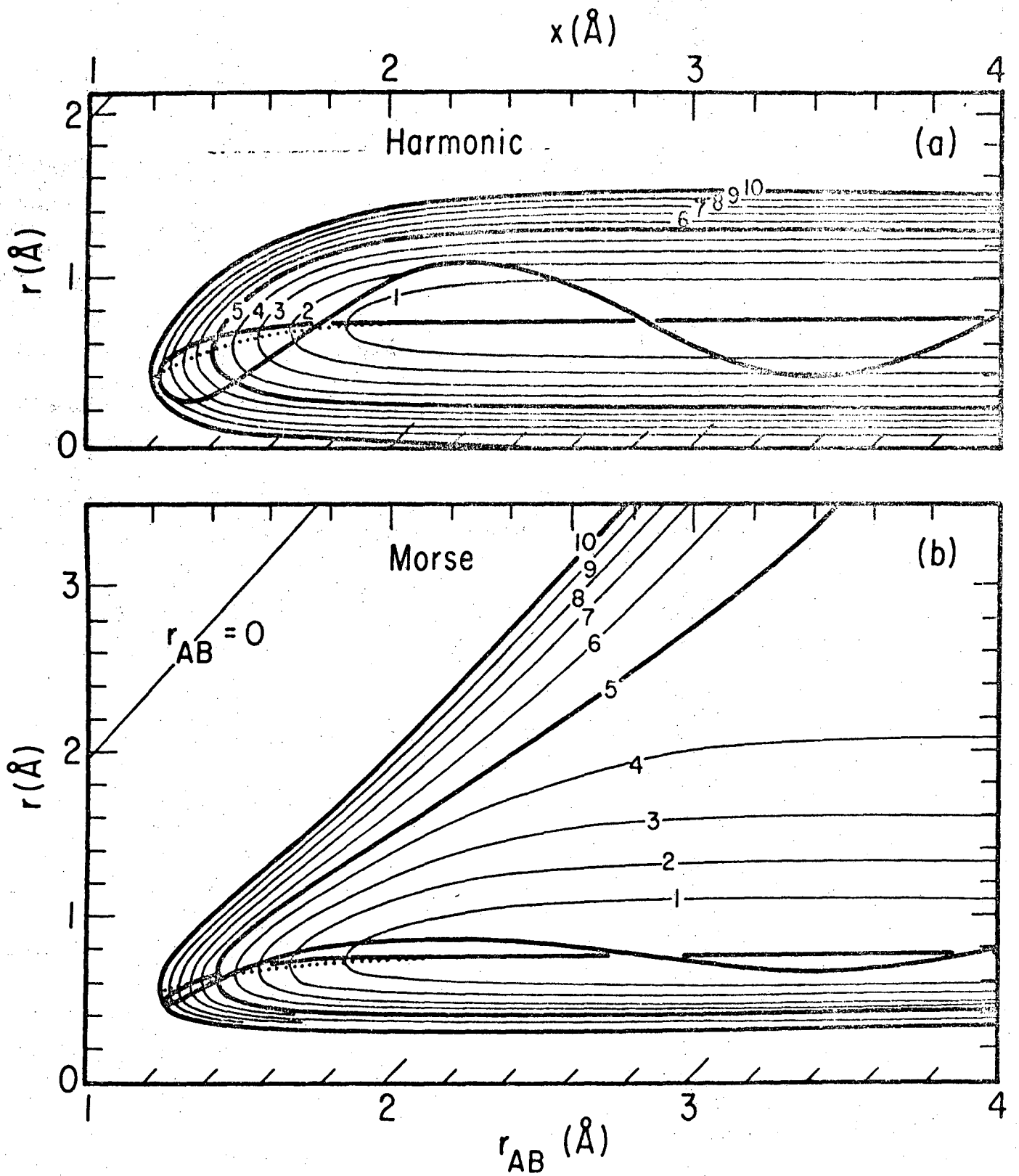

XBL 7311-5582

Fig. 5

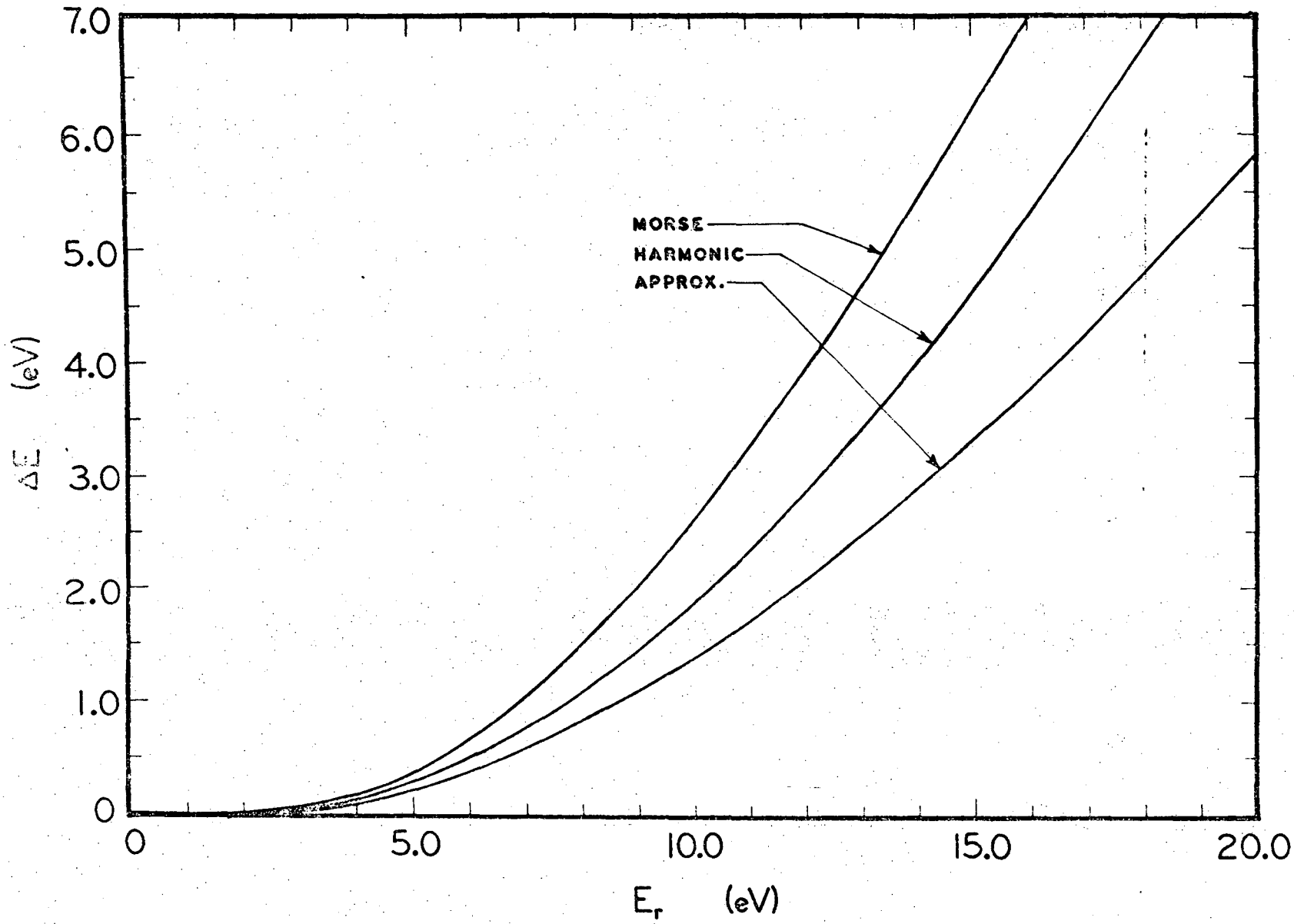

XBL 737-1546

Fig. 6

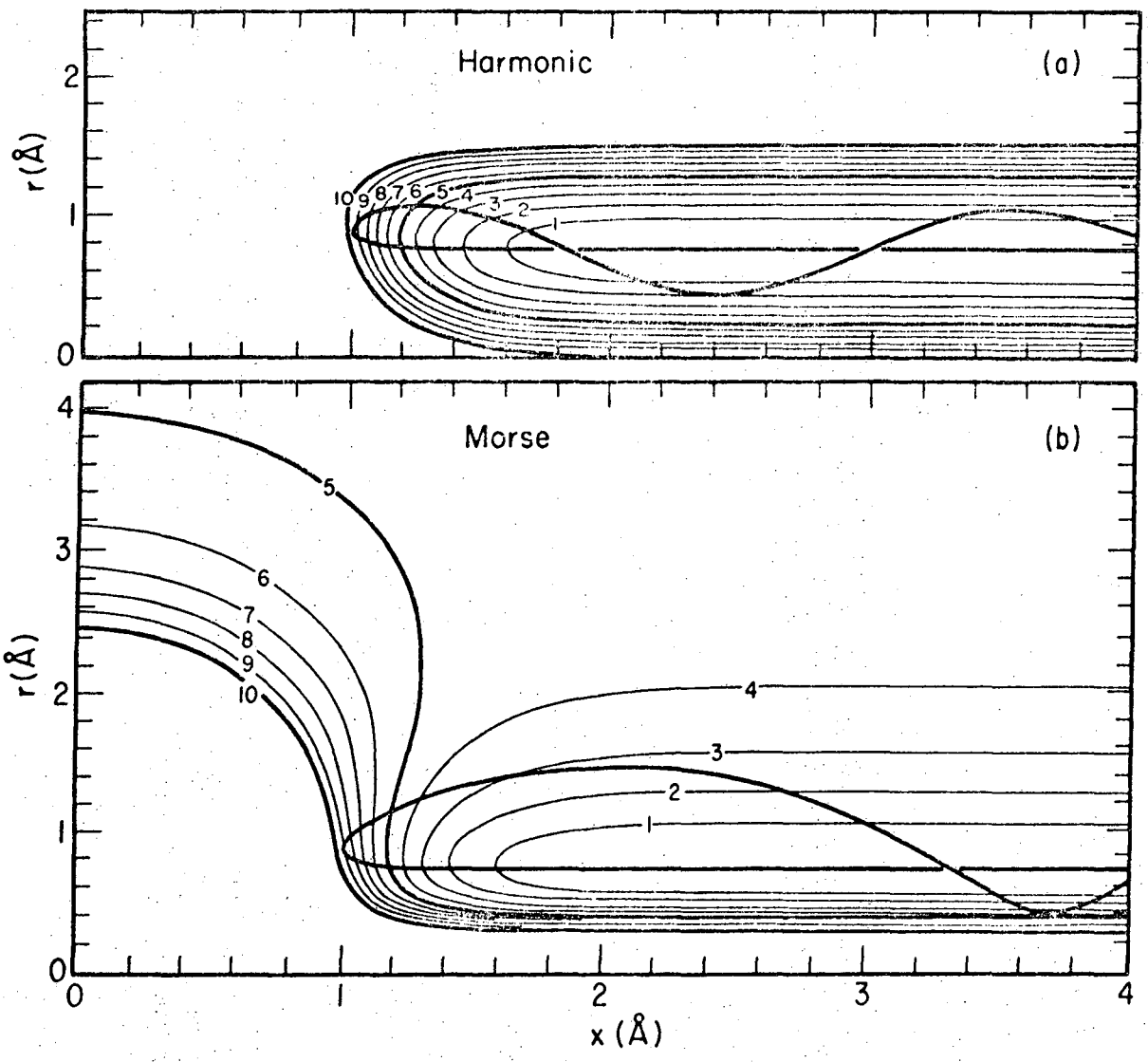
Harmonic
(a)
r(Å)
10 9 8 7 6 5 4 3 2 1
Morse
(b)
r(Å)
5
6
7
8
9
10
4
3
2
1
x (Å)
XBL 7311-5583

Fig. 7

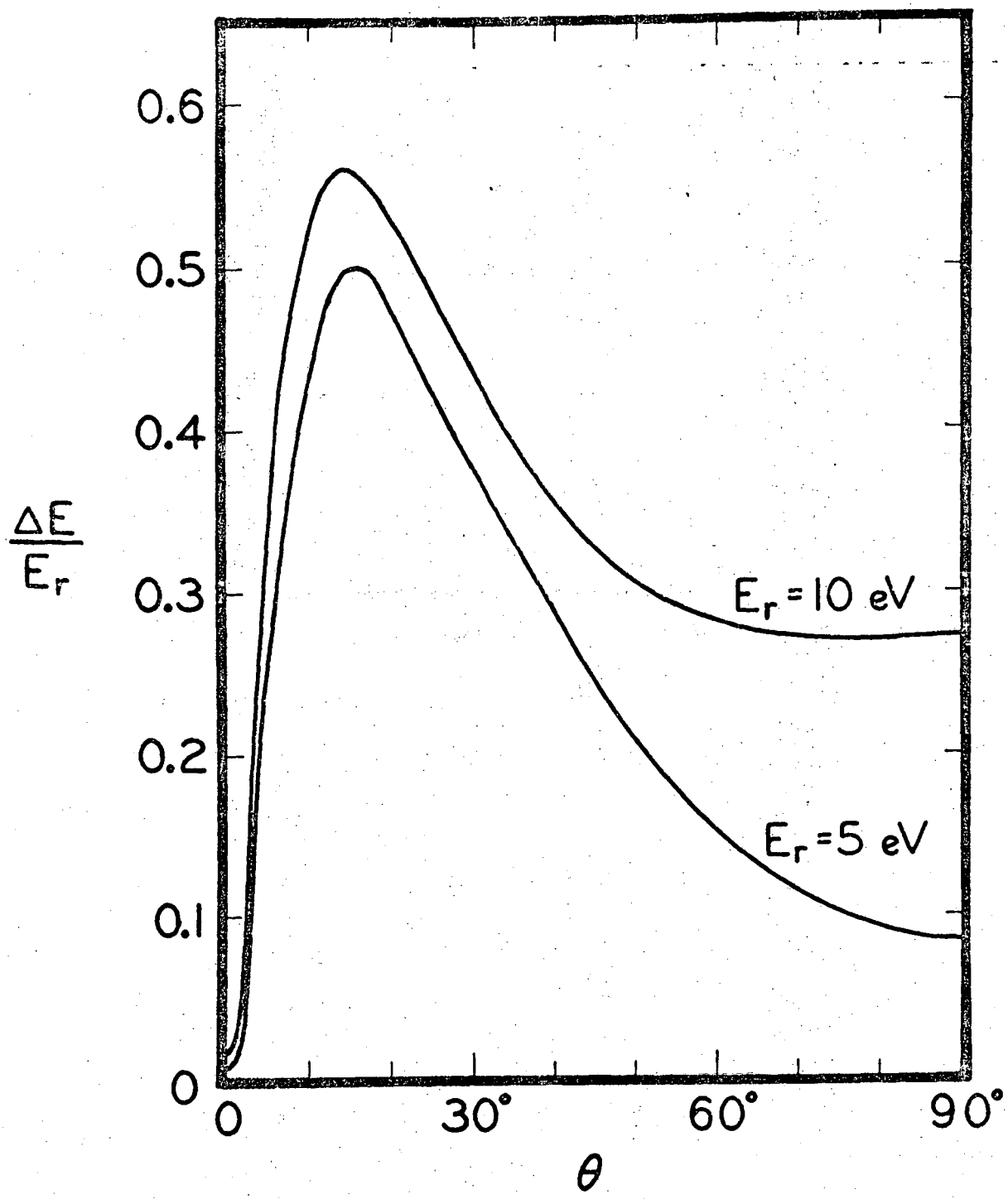

XBL 737-1533

Fig. 8

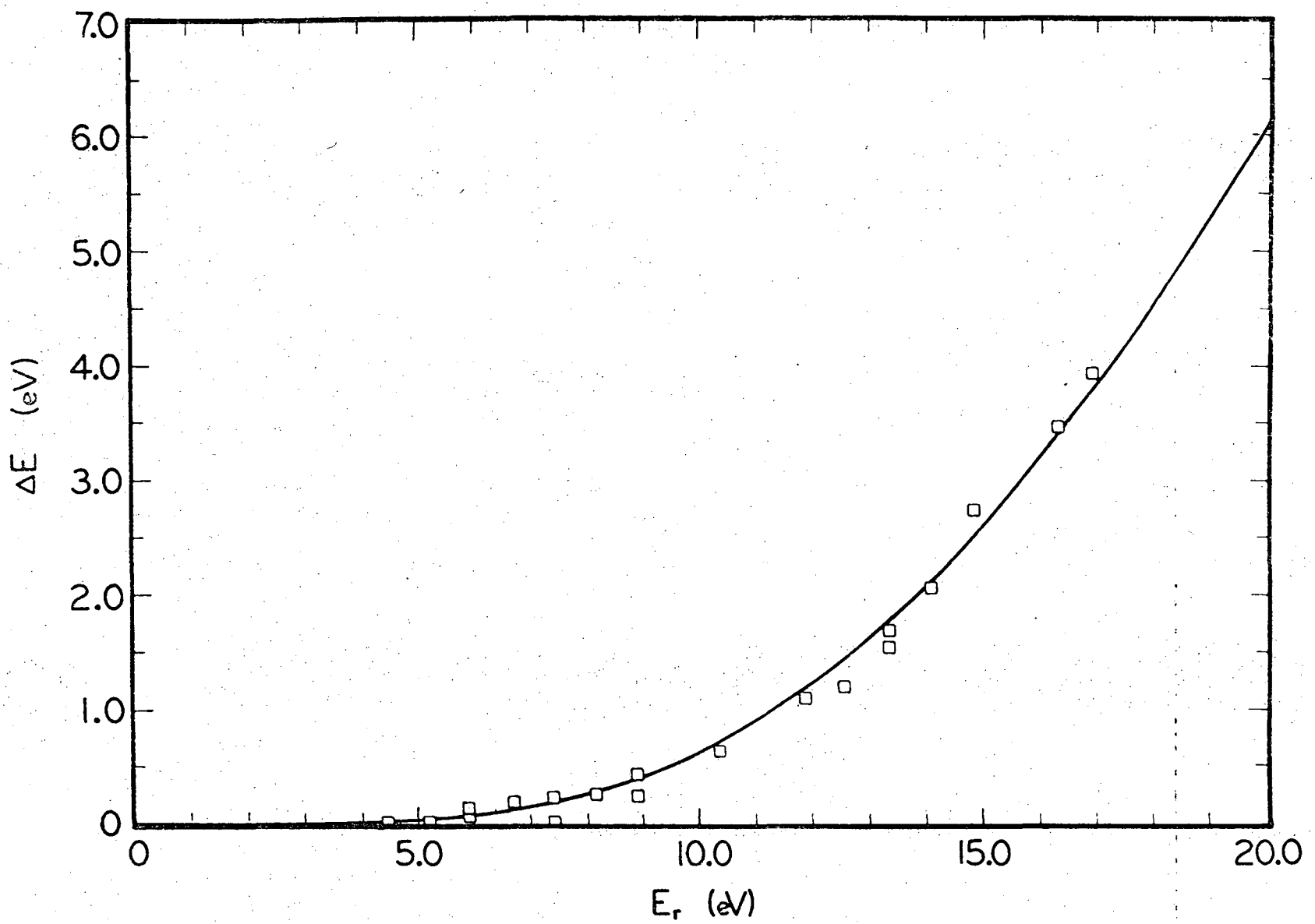

XBL 737-1542

Fig. 9

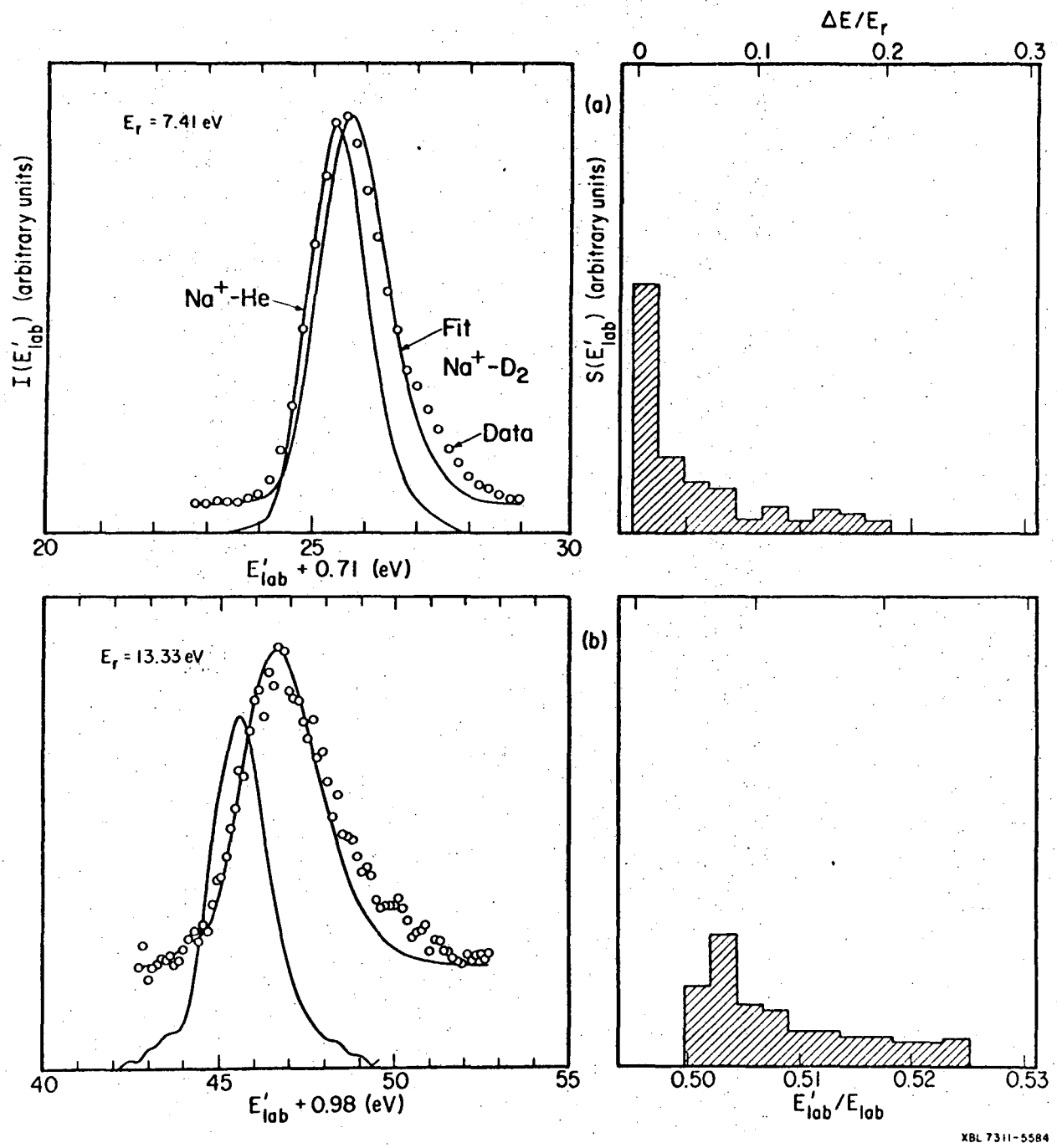
ΔE/E_r
0
0.1
0.2
0.3
(a)
E_r = 7.41 eV
I(E'_lab) (arbitrary units)
S(E'_lab) (arbitrary units)
Na+-He
Fit
Na+-D2
Data
20
25
30
E'_lab + 0.71 (eV)
(b)
E_r = 13.33 eV
40
45
50
55
E'_lab + 0.98 (eV)
0.50
0.51
0.52
0.53
E'_lab/E_lab
XBL 7311-5584

Fig. 10

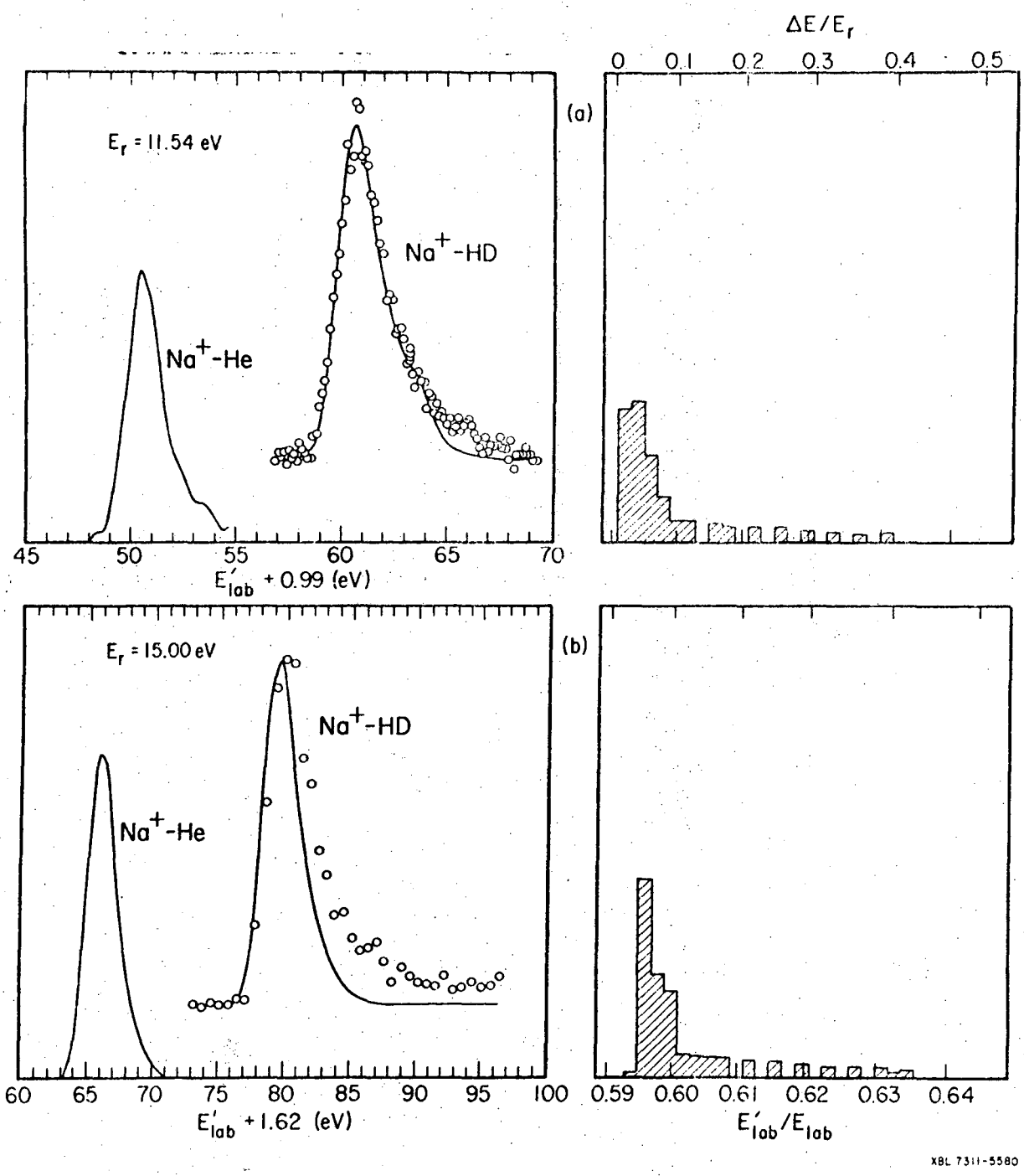
ΔE/E_r
0 0.1 0.2 0.3 0.4 0.5
(a)
E_r = 11.54 eV
Na+-HD
Na+-He
45 50 55 60 65 70
E'_lab + 0.99 (eV)
(b)
E_r = 15.00 eV
Na+-HD
Na+-He
60 65 70 75 80 85 90 95 100
E'_lab + 1.62 (eV)
0.59 0.60 0.61 0.62 0.63 0.64
E'_lab/E_lab
XBL 7311-5580

Fig. 11

LEGAL NOTICE

This report was prepared as an account of work sponsored by the United States Government. Neither the United States nor the United States Atomic Energy Commission, nor any of their employees, nor any of their contractors, subcontractors, or their employees, makes any warranty, express or implied, or assumes any legal liability or responsibility for the accuracy, completeness or usefulness of any information, apparatus, product or process disclosed, or represents that its use would not infringe privately owned rights.

TECHNICAL INFORMATION DIVISION
LAWRENCE BERKELEY LABORATORY
UNIVERSITY OF CALIFORNIA
BERKELEY, CALIFORNIA 94720